LETTER

doi:10.1038/nature14360

Lunar tungsten isotopic evidence for the late veneer

Thomas S. Kruijer[1], Thorsten Kleine[1], Mario Fischer-Gödde[1] & Peter Sprung[1]†

According to the most widely accepted theory of lunar origin, a giant impact on the Earth led to the formation of the Moon, and also initiated the final stage of the formation of the Earth's core[1]. Core formation should have removed the highly siderophile elements (HSE) from Earth's primitive mantle (that is, the bulk silicate Earth), yet HSE abundances are higher than expected[2]. One explanation for this overabundance is that a 'late veneer' of primitive material was added to the bulk silicate Earth after the core formed[2]. To test this hypothesis, tungsten isotopes are useful for two reasons: first, because the late veneer material had a different $^{182}W/^{184}W$ ratio to that of the bulk silicate Earth, and second, proportionally more material was added to the Earth than to the Moon[3]. Thus, if a late veneer did occur, the bulk silicate Earth and the Moon must have different $^{182}W/^{184}W$ ratios. Moreover, the Moon-forming impact would also have created ^{182}W differences because the mantle and core material of the impactor with distinct $^{182}W/^{184}W$ would have mixed with the proto-Earth during the giant impact. However the $^{182}W/^{184}W$ of the Moon has not been determined precisely enough to identify signatures of a late veneer or the giant impact. Here, using more-precise measurement techniques, we show that the Moon exhibits a ^{182}W excess of 27 ± 4 parts per million over the present-day bulk silicate Earth. This excess is consistent with the expected ^{182}W difference resulting from a late veneer with a total mass and composition inferred from HSE systematics[2]. Thus, our data independently show that HSE abundances in the bulk silicate Earth were established after the giant impact and core formation, as predicted by the late veneer hypothesis. But, unexpectedly, we find that before the late veneer, no ^{182}W anomaly existed between the bulk silicate Earth and the Moon, even though one should have arisen through the giant impact. The origin of the homogeneous ^{182}W of the pre-late-veneer bulk silicate Earth and the Moon is enigmatic and constitutes a challenge to current models of lunar origin.

The extinct ^{182}Hf–^{182}W system (half-life, 8.9 Myr) is a versatile tool for investigating potential isotopic differences between the Earth and Moon because it is sensitive to different degrees of metal–silicate equilibration during core formation, to mixing processes during the giant impact, and to the addition of meteoritic material to silicate mantles after the giant impact. During core formation, the lithophile Hf is fractionated from the siderophile W, and the resulting distinct Hf/W ratio causes the mantle and the core to have different values of $\varepsilon^{182}W$ (that is, the deviation in parts per 10,000 of the $^{182}W/^{184}W$ ratio from the value of the present-day bulk silicate Earth), depending on the timescales and conditions of core formation[4]. This makes $\varepsilon^{182}W$ a sensitive tracer of proto-Earth and impactor components in the Moon, as well as of the late accretion of chondritic, ^{182}W-depleted material that was added to the mantles of the Earth and Moon. For instance, small ^{182}W excesses in some Archaean terrestrial rocks may reflect mantle sources that lack a portion of the late veneer[5], although such ^{182}W heterogeneities may also result from early mantle differentiation processes[6]. As the fraction of late-accreted mass added to the lunar mantle was much smaller than the fraction added to the bulk silicate Earth (BSE)[3,7], mass balance calculations suggest that the late veneer would inevitably have generated an Earth–Moon ^{182}W difference[8]. A $\varepsilon^{182}W$ difference between the Moon and the BSE may also exist because, during the giant impact that gave rise to the Moon, different proportions of the impactor material, which had distinct $\varepsilon^{182}W$, ended up in the Earth and the Moon. Therefore, identifying a difference of $\varepsilon^{182}W$ (or lack thereof) between the Earth and Moon would provide key information regarding the earliest history of the Earth–Moon system; such information would constrain the process and timing of late accretion and help shape models of lunar origin.

However, determining the lunar $\varepsilon^{182}W$ is complicated by cosmic-ray-induced secondary neutron capture reactions. These reactions not only involve ^{182}W production via neutron capture by ^{181}Ta, but also neutron-capture-induced burnout of ^{182}W (ref. 9). Hence, the previously measured value of $\varepsilon^{182}W = 0.09 \pm 0.10$ (2 standard error, s.e.) for the Moon[10], which was based on Ta-free and thus cosmogenic-^{182}W-free lunar metals, may have been lowered by ^{182}W burnout, and therefore only provides a minimum estimate. Without a suitable neutron dosimeter, the previously measured $\varepsilon^{182}W$ values of the lunar metals had been corrected using cosmic ray exposure ages[10,11], but these do not directly measure the neutron dose that affects W isotopes. Furthermore, the analytical precision of the previous studies was >10 p.p.m. (2 s.e.) for individual samples, which is insufficient to resolve a (hypothetical) small ^{182}W anomaly of the Moon. Consequently, it has been unclear until now whether the Moon and the present-day BSE differ significantly in $\varepsilon^{182}W$.

In this study, we determined the $\varepsilon^{182}W$ of the Moon using improved analytical techniques for high-precision W isotope measurements[12] combined with a new approach to quantifying cosmogenic $\varepsilon^{182}W$ variations using Hf isotopes[13]. All investigated samples are impact rocks (see ref. 14 and references therein), so their $\varepsilon^{182}W$ may have been modified through the addition of meteoritic material. We determined the magnitude of such meteorite contamination from the abundances of HSE in the investigated samples[15,16], producing corrections of ~0.04 $\varepsilon^{182}W$ for samples 68115 and 68815, and of less than ~0.02 $\varepsilon^{182}W$ for all other samples (Table 1). We focused on KREEP-rich samples because they have a near-constant Ta/W ratio (ref. 11), implying essentially invariant effects on $\varepsilon^{182}W$ for a given neutron dose (KREEP is thought to represent the residual liquid of the lunar magma ocean and is enriched in incompatible elements including potassium, K, rare-earth elements, REE, and phosphorus, P). The KREEP-rich samples exhibit a well-defined $\varepsilon^{182}W$–$\varepsilon^{180}Hf$ correlation (Fig. 1), reflecting the fact that Ta, W and Hf isotopes are most sensitive to neutrons of similar (epithermal) energies. All investigated KREEP-rich samples have a common pre-exposure $\varepsilon^{182}W$ (that is, unaffected by neutron capture) of $+0.27 \pm 0.04$ (95% confidence interval) defined either by the intercept of the $\varepsilon^{182}W$–$\varepsilon^{180}Hf$ correlation (Fig. 1) or by samples lacking significant $\varepsilon^{180}Hf$ anomalies (samples 14321, 68115, 68815; Fig. 2). We interpret the pre-exposure $\varepsilon^{182}W$ of the KREEP-rich samples to represent that of the bulk silicate Moon, because lunar differentiation at ~4.4 Gyr ago (Ga; refs 13, 17, 18) was too late to produce ^{182}W variations within the Moon, consistent with the indistinguishable $\varepsilon^{182}W$ of non-irradiated mare basalts[13] and KREEP (see Methods). Our newly determined pre-exposure $\varepsilon^{182}W$

[1]Institut für Planetologie, Westfälische Wilhelms-Universität Münster, Wilhelm-Klemm-Strasse 10, D-48149 Münster, Germany. †Present address: Universität zu Köln, Institut für Geologie und Mineralogie, Zülpicher Strasse 49b, D-50674 Köln, Germany.

Table 1 | Tungsten and Hf isotope data for KREEP-rich samples analysed by MC-ICPMS

Sample	t_{CRE} § (Ma)	*N*	$\varepsilon^{182/184}W\ (6/4)_{meas.}$* (±2σ)	$\varepsilon^{182/184}W\ (6/4)_{corr.}$† (±2σ)	W_{met}‡ (%)[c]	$\varepsilon^{180}Hf$ (±95% confidence interval)
Weakly irradiated samples						
14321, 1827		2	0.29±0.10	0.29±0.10	0.1	−0.02±0.08
14321, 1856		6	0.27±0.05	0.27±0.05	0.1	−0.02±0.08
14321 (weighted mean)	23.8		0.27±0.04	0.27±0.04	0.1	
68115, 295		4	0.24±0.06	0.28±0.06	1.4	0.02±0.13
68115, 112		3	0.27±0.10	0.31±0.10	1.4	0.02±0.13
68115 (weighted mean)	2.08		0.25±0.05	0.29±0.05	1.4	
68815, 400	2.04	2	0.18±0.10	0.21±0.10	1.0	−0.03±0.16
14321, 68115, 68815 (weighted mean)			0.25±0.03	0.27±0.03		
Strongly irradiated samples						
14163, 921	NA	5	2.35±0.04	ND	ND	−3.79±0.08
12034, 120	NA	3	1.26±0.10	ND	ND	−1.79±0.09
14310, 676	259	3	1.87±0.10	ND	ND	−2.94±0.08
62235, 122	153	2	1.63±0.10	ND	ND	−2.46±0.10

All Hf isotope data are from ref. 13, except for samples 14321 and 14163 which were newly analysed (see Methods). *N*, number of measurements of each sample; NA, not available; ND, not determined.
* Measured $\varepsilon^{182}W$ internally normalized to $^{186}W/^{184}W = 0.92767$, denoted by (6/4).
† $\varepsilon^{182}W$ corrected for meteoritic contamination on the lunar surface using measured HSE and W abundances (see Methods).
‡ Percentage of W in sample that derives from meteoritic impactor component added at lunar surface.
§ Cosmic-ray exposure ages (t_{CRE}) of lunar samples (ref. 14 and references therein).

of +0.27 ± 0.04 is significantly higher than the previously obtained mean value of 0.09 ± 0.10 for lunar metal samples (ref. 10), but for non-irradiated samples (68115, 68815) there is good agreement between our data and previous data (Fig. 2). For more strongly irradiated samples, however, the $\varepsilon^{182}W$ of the metals tends to be slightly lower[10], resulting in an overall decrease of the mean $\varepsilon^{182}W$ inferred from the lunar metals. Therefore, the higher pre-exposure $\varepsilon^{182}W$ of +0.27 ± 0.04 determined here reflects not only the better precision of our measurements, but also that the previous study[10] did not fully quantify neutron capture effects in the metals.

The well-resolved ^{182}W excess of the Moon compared to the present-day BSE (Fig. 2) places important constraints on the occurrence, mass and timing of the late veneer as well as on the origin of the Moon. Below we first evaluate the magnitude of any $\varepsilon^{182}W$ difference between the BSE and the Moon induced by the late veneer, and then we assess whether there is a resolvable ^{182}W anomaly in the Moon resulting from the mixing of impactor and proto-Earth material during the giant impact. The mass and composition of the late veneer is constrained through absolute and relative HSE abundances and ratios of S, Se and Te in Earth's primitive mantle[2,19,20]. On this basis, the late veneer probably had a carbonaceous-chondrite-like composition with a minor fraction of iron-meteorite-like material[16], corresponding to ~0.35% of Earth's mass. This composition can explain several geochemical signatures of the Earth's mantle, including its chondritic Os/Ir, Pt/Ir and Rh/Ir but suprachondritic Ru/Ir and Pd/Ir, as well as its $^{187}Os/^{188}Os$ value[2] and Se–Te systematics[19]. Mass balance considera-

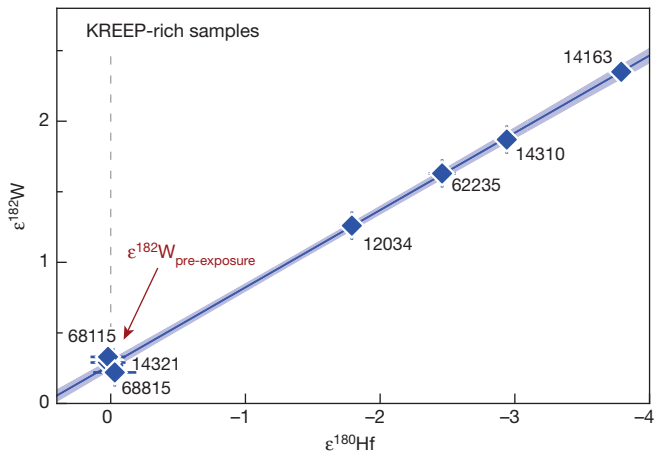

Figure 1 | Plot of $\varepsilon^{182}W$ versus $\varepsilon^{180}Hf$ determined for KREEP-rich samples. $\varepsilon^{182}W$ has been internally normalized to $^{186}W/^{184}W = 0.92767$: elsewhere this is referred to as $\varepsilon^{182}W$ (6/4) (see Methods and Table 1). Solid line is a best-fit linear regression through the data (slope = −0.549 ± 0.019; MSWD = 0.36) with the intersection at $\varepsilon^{180}Hf = 0$ (arrowed) defining the pre-exposure $\varepsilon^{182}W$ (= +0.27 ± 0.04, ±95% confidence interval). Error bars, external uncertainties (95% confidence interval or 2 s.d.; Extended Data Table 2).

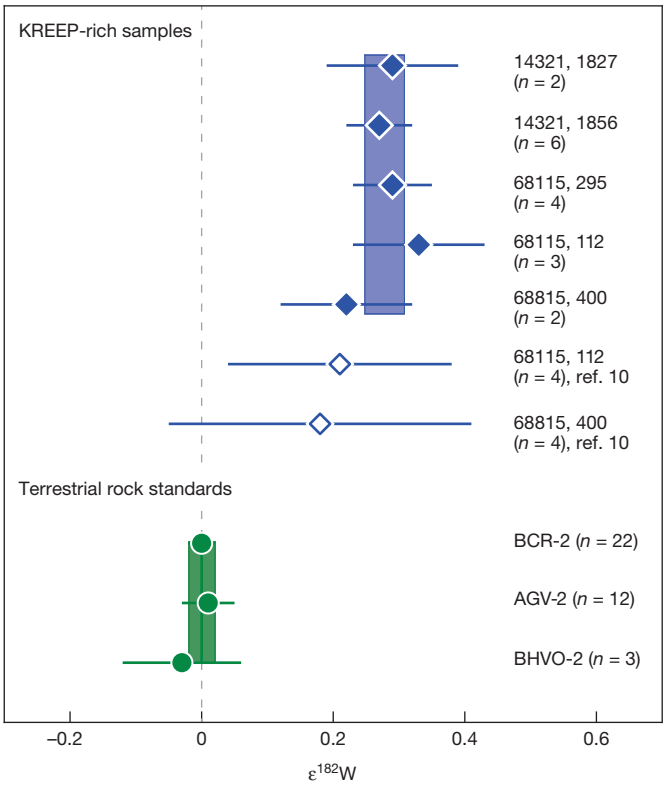

Figure 2 | $\varepsilon^{182}W$ data of KREEP-rich samples and terrestrial rock standards. Top panel, data from this study (filled symbols) and for metal samples from ref. 10 (open symbols). Data points of 68115 and 68815 (this study) were corrected for a minor contribution from meteoritic contamination at the lunar surface (Table 1). Error bars indicate external uncertainties derived from the 2 s.d. obtained for terrestrial rock standards analysed in this study (if $N < 4$) or 95% confidence interval of multiple solution replicates of a sample (if $N \geq 4$) (Extended Data Table 1). Bottom panel, data from terrestrial rock standards. Top panel, weighted mean ($n = 5$) $\varepsilon^{182}W = +0.27 \pm 0.03$ (95% confidence interval, blue shaded area); bottom panel, mean $\varepsilon^{182}W$ ($n = 37$) = 0.00 ± 0.10 (2 s.d.) = 0.00 ± 0.02 (95% confidence interval, green shaded area). $\varepsilon^{182}W$ has been internally normalized to $^{186}W/^{184}W = 0.92767$, and dashed grey line shows $\varepsilon^{182}W = 0$.

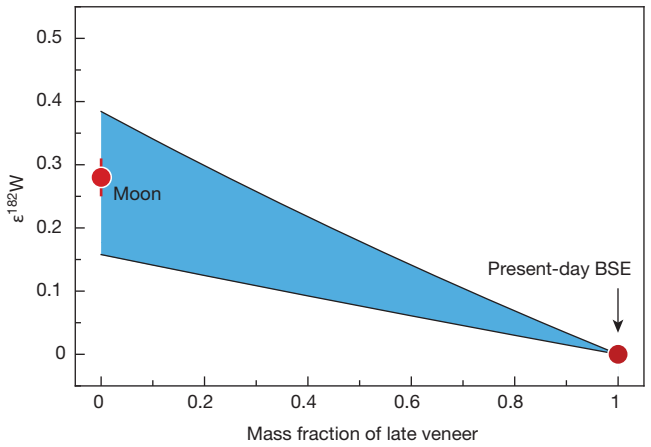

Figure 3 | Plot of ε^{182}W versus mass fraction of late-accreted material on Earth. Mass balance calculations (blue envelope) predict a positive ε^{182}W signature if the full complement of late accretion is subtracted from the present-day BSE composition (right red circle, $\varepsilon^{182}W \equiv 0$), in excellent agreement with the lunar ε^{182}W value (left red circle; $\varepsilon^{182}W = +0.27 \pm 0.04$, 95% confidence interval). The uncertainty on the pre-late veneer ε^{182}W of the BSE mainly results from the uncertainty on the W concentration of the BSE (13 ± 5 p.p.b.). For details about the late veneer composition used in the mass balance, see Methods.

tions imply that the addition of a late veneer of this composition lowered the ε^{182}W of the BSE by $+0.22^{+0.16}_{-0.06}$ (Fig. 3), where this estimate's uncertainty mainly comes from that of the W concentration of the BSE. A late veneer composed exclusively of known groups of chondrites would have resulted in an only slightly smaller but still consistent shift of ~0.1 to ~0.3 ε^{182}W (see Methods). The corresponding effect of the late veneer on the lunar ε^{182}W is negligible, given that the mass fraction added to the lunar mantle was an order of magnitude smaller than that added to the Earth[3,7]. Therefore, the ε^{182}W difference between the Moon and the present-day BSE of $+0.27 \pm 0.04$ can be entirely accounted for by the addition of ^{182}W-depleted material to the BSE during late accretion, with a total mass consistent with that derived from the HSE abundances in Earth's mantle[2,16] (Fig. 3). This implies that previously accumulated HSEs in the Earth's mantle had been sequestered into Earth's core during the giant impact[8], demonstrating that the entire late veneer was added after the giant impact and the final stages of core segregation. These ^{182}W results therefore provide independent evidence for the late veneer hypothesis by demonstrating that the HSE abundances in the Earth's mantle were established by addition of primitive material after the Earth's core formed.

The close agreement between the predicted late-veneer-induced ε^{182}W shift and that observed between the BSE and the Moon suggests that, before addition of the late veneer, the BSE and the Moon had indistinguishable values of ε^{182}W. This implies that there is no resolvable radiogenic ^{182}W difference between the Moon and the Earth, probably because the Moon formed late[10,18,21]—when ^{182}Hf was already extinct—or perhaps because the BSE and the silicate Moon have very similar Hf/W. In addition, the data suggest that the giant impact did not induce a resolvable ^{182}W anomaly in the Moon. This is consistent with the Earth–Moon isotopic homogeneity observed for Ti (ref. 22), Si (ref. 23) and O (ref. 24). We note that a small O isotope difference exists between the Moon and the present-day BSE and this is most probably caused by late accretion, because the late veneer was probably dominated by carbonaceous-chondrite-like material (see above) and, consequently, had a distinctly lower Δ^{17}O than the Earth and Moon. Thus, addition of a late veneer with this composition and a mass as derived from HSE and ^{182}W systematics would have led to the observed Earth–Moon difference in Δ^{17}O (ref. 24). So as is the case for ε^{182}W, once the effect of late accretion is taken into account, the pre-late-veneer BSE and the Moon have indistinguishable Δ^{17}O.

The Earth–Moon isotopic homogeneity for Ti, Si and O may mean that the Earth and the impactor accreted from a homogeneous inner-disk reservoir[25] or that the Moon formed either from proto-Earth mantle material[26,27], or from equal portions of the mantles of two colliding half-Earths[28]. However, in both cases, the homogeneous ε^{182}W of the pre-late-veneer BSE and the Moon is not easily explained, because the giant impact would have modified the ε^{182}W of proto-Earth's mantle in two ways: (1) by adding the impactor mantle material, which presumably had distinct ε^{182}W, and (2) through the (partial) equilibration of the impactor core with the proto-Earth's mantle. As such, the pre-giant-impact ε^{182}W of the Earth's mantle was most probably different from its post-giant-impact value, meaning that making the Moon out of the proto-Earth's mantle would probably not result in a homogeneous ε^{182}W of the pre-late-veneer BSE and the Moon (Extended Data Fig. 3). Moreover, the lunar accretion disk probably would have contained W-rich but ^{182}W-depleted impactor core material[1,26,28], which consequently would have generated a significant shift in the W isotope composition of the proto-lunar material (Extended Data Fig. 4). Thus, although specific impactor compositions, proto-Earth compositions, and impact conditions that could produce a similar ^{182}W composition of the pre-late-veneer BSE and the Moon can be identified[25], it is far more likely that significant Earth–Moon ε^{182}W differences were produced, even if the Moon predominantly consists of proto-Earth material. Consequently, it would take extraordinary circumstances to generate the Earth–Moon ε^{182}W homogeneity through simple mixing of proto-Earth and impactor material during the giant impact.

The ε^{182}W homogeneity might be accounted for by post-giant-impact equilibration via a shared atmosphere of the lunar accretion disk and the Earth's mantle[29], but this would be difficult for a refractory element like W (ref. 22). Other possible origins of the ε^{182}W homogeneity might be that the Moon was formed through impact-triggered fission from a fast-spinning proto-Earth[26] or that efficient equilibration occurred during the collision of two half-Earths[28]. However, in the last two scenarios it still has to be evaluated whether equilibration between the impactor and the proto-Earth would be possible before ejection of the proto-lunar material. Either way, the Earth–Moon ^{182}W homogeneity constitutes a fundamental constraint on any successful model of lunar origin.

Online Content Methods, along with any additional Extended Data display items and Source Data, are available in the online version of the paper; references unique to these sections appear only in the online paper.

Received 5 December 2014; accepted 25 February 2015.
Published online 8 April 2015.

1. Canup, R. M. & Asphaug, E. Origin of the Moon in a giant impact near the end of the Earth's formation. *Nature* **412,** 708–712 (2001).
2. Walker, R. J. Highly siderophile elements in the Earth, Moon and Mars: update and implications for planetary accretion and differentiation. *Chem. Erde Geochem.* **69,** 101–125 (2009).
3. Day, J. M. D., Pearson, D. G. & Taylor, L. A. Highly siderophile element constraints on accretion and differentiation of the Earth-Moon system. *Science* **315,** 217–219 (2007).
4. Kleine, T. *et al.* Hf–W chronology of the accretion and early evolution of asteroids and terrestrial planets. *Geochim. Cosmochim. Acta* **73,** 5150–5188 (2009).
5. Willbold, M., Elliott, T. & Moorbath, S. The tungsten isotopic composition of the Earth's mantle before the terminal bombardment. *Nature* **477,** 195–198 (2011).
6. Touboul, M., Puchtel, I. S. & Walker, R. J. ^{182}W evidence for long-term preservation of early mantle differentiation products. *Science* **335,** 1065–1069 (2012).
7. Day, J. M. D., Walker, R. J., James, O. B. & Puchtel, I. S. Osmium isotope and highly siderophile element systematics of the lunar crust. *Earth Planet. Sci. Lett.* **289,** 595–605 (2010).
8. Walker, R. J. Siderophile element constraints on the origin of the Moon. *Phil. Trans. R. Soc. A* **372,** http://dx.doi.org/10.1098/rsta.2013.0258 (2014).
9. Leya, I., Wieler, R. & Halliday, A. N. Cosmic-ray production of tungsten isotopes in lunar samples and meteorites and its implications for Hf–W cosmochemistry. *Earth Planet. Sci. Lett.* **175,** 1–12 (2000).
10. Touboul, M., Kleine, T., Bourdon, B., Palme, H. & Wieler, R. Late formation and prolonged differentiation of the Moon inferred from W isotopes in lunar metals. *Nature* **450,** 1206–1209 (2007).
11. Kleine, T., Palme, H., Mezger, K. & Halliday, A. N. Hf-W chronometry of lunar metals and the age and early differentiation of the Moon. *Science* **310,** 1671–1674 (2005).

12. Kruijer, T. S. *et al.* Protracted core formation and rapid accretion of protoplanets. *Science* **344,** 1150–1154 (2014).
13. Sprung, P., Kleine, T. & Scherer, E. E. Isotopic evidence for chondritic Lu/Hf and Sm/Nd of the Moon. *Earth Planet. Sci. Lett.* **380,** 77–87 (2013).
14. Meyer, C. The Lunar Sample Compendium. Available at http://curator.jsc.nasa.gov/Lunar/lsc/index.cfm (20 May 2013).
15. Morgan, J. W., Ganapathy, R., Higuchi, H., Krähenbühl, U. & Anders, E. Lunar basins: tentative characterization of projectiles, from meteoritic elements in Apollo 17 boulders. *Proc. Lunar Planet. Sci. Conf.* **2,** 1703–1736 (1974).
16. Fischer-Gödde, M. & Becker, H. Osmium isotope and highly siderophile element constraints on ages and nature of meteoritic components in ancient lunar impact rocks. *Geochim. Cosmochim. Acta* **77,** 135–156 (2012).
17. Gaffney, A. M. & Borg, L. E. A young solidification age for the lunar magma ocean. *Geochim. Cosmochim. Acta* **140,** 227–240 (2014).
18. Carlson, R. W., Borg, L. E., Gaffney, A. M. & Boyet, M. Rb-Sr, Sm-Nd and Lu-Hf isotope systematics of the lunar Mg-suite: the age of the lunar crust and its relation to the time of Moon formation. *Phil. Trans. R. Soc. A* 372, http://dx.doi.org/10.1098/rsta.2013.024 (2014).
19. Wang, Z. & Becker, H. Ratios of S, Se and Te in the silicate Earth require a volatile-rich late veneer. *Nature* **499,** 328–331 (2013).
20. Becker, H. *et al.* Highly siderophile element composition of the Earth's primitive upper mantle: constraints from new data on peridotite massifs and xenoliths. *Geochim. Cosmochim. Acta* **70,** 4528–4550 (2006).
21. Borg, L. E., Connelly, J. N., Boyet, M. & Carlson, R. W. Chronological evidence that the Moon is either young or did not have a global magma ocean. *Nature* **477,** 70–72 (2011).
22. Zhang, J., Dauphas, N., Davis, A. M., Leya, I. & Fedkin, A. The proto-Earth as a significant source of lunar material. *Nature Geosci.* **5,** 251–255 (2012).
23. Armytage, R. M. G., Georg, R. B., Williams, H. M. & Halliday, A. N. Silicon isotopes in lunar rocks: implications for the Moon's formation and the early history of the Earth. *Geochim. Cosmochim. Acta* **77,** 504–514 (2012).
24. Herwartz, D., Pack, A., Friedrichs, B. & Bischoff, A. Identification of the giant impactor Theia in lunar rocks. *Science* **344,** 1146–1150 (2014).
25. Dauphas, N., Burkhardt, C., Warren, P. & Teng, F.-Z. Geochemical arguments for an Earth-like Moon-forming impactor. *Phil. Trans. R. Soc. A* http://dx.doi.org/10.1098/rsta.2013.0244 (2014).
26. Ćuk, M. & Stewart, S. T. Making the Moon from a fast-spinning Earth: a giant impact followed by resonant despinning. *Science* **338,** 1047–1052 (2012).
27. Reufer, A., Meier, M. M. M., Benz, W. & Wieler, R. A hit-and-run giant impact scenario. *Icarus* **221,** 296–299 (2012).
28. Canup, R. M. Forming a Moon with an Earth-like composition via a giant impact. *Science* **338,** 1052–1055 (2012).
29. Pahlevan, K. & Stevenson, D. J. Equilibration in the aftermath of the lunar-forming giant impact. *Earth Planet. Sci. Lett.* **262,** 438–449 (2007).

Acknowledgements We thank CAPTEM, NASA and R. Zeigler for providing the Apollo lunar samples for this study. We thank G. Brügmann for providing an HSE spike. C. Brennecka is acknowledged for comments on the paper, and we also thank A. Brandon for comments.

Author Contributions T.S.K. prepared the lunar samples for W isotope analyses and performed the measurements. All authors contributed to the interpretation of the data and preparation of the manuscript.

Author Information Reprints and permissions information is available at www.nature.com/reprints. The authors declare no competing financial interests. Readers are welcome to comment on the online version of the paper. Correspondence and requests for materials should be addressed to T.S.K. (thomas.kruijer@wwu.de).

METHODS

Sample preparation and chemical separation of W. Seven KREEP-rich whole rock samples that span a wide range in cosmic ray exposure ages were selected for this study (12034, 14163, 14310, 14321, 62235, 68115, 68815)[14]. The Hf isotope compositions of these samples had been determined by us previously[13]. Only the Hf isotope compositions of samples 14321 and 14163 were newly measured (Table 1) by the same methods used in the previous study[13]. Note that all lunar ε^{180}Hf and ε^{178}Hf data are given relative to the average composition obtained for terrestrial rock standards. For W isotope analyses, samples received as rock fragments were ultrasonically cleaned and rinsed with ethanol, and then carefully crushed and ground to a fine powder in an agate mortar. Combined W and Hf isotope compositions were determined on separate splits of the same powder aliquots (~0.2 g). From three samples with no resolvable Hf isotope anomaly (68115, 68815, 14321) more material (~0.9 g) was powdered for additional W isotope measurements. The analytical techniques for sample digestion, chemical separation of W, and W isotope ratio measurements by MC-ICPMS (Multi Collector Inductively Coupled Plasma Mass Spectrometry) are based on our previously developed procedures[12,30]. The KREEP-rich samples and terrestrial rock standards were dissolved by table-top digestion in ~20 ml HF–HNO_3 (2:1) at 130–150 °C for 2–3 days. After digestion, samples were evaporated to dryness at 130 °C, and then concentrated HNO_3-HCl was added repeatedly to the samples to remove fluoride precipitates. Subsequently, the samples were converted through repeated evaporations to dryness in 6 M HCl–0.06 M HF. Finally, the samples were completely dissolved in 25 ml 6 M HCl–0.06 M HF. For three weakly irradiated samples (BL01-03) approximately 1–10% aliquots (equivalent to ~2–4 ng W) of these 6 M HCl–0.06 M HF solutions were spiked with a mixed ^{180}Hf–^{183}W tracer that was calibrated against pure Hf and W metal standards[31]. Tungsten was separated from the sample matrix using a two-stage anion exchange chromatography technique that was slightly modified from previously published methods[30–33]. All spike-free fractions were evaporated to dryness and re-dissolved in 25 ml 0.5 M HCl–0.5 M HF before loading onto the first anion exchange column (4 ml BioRad AG1 × 8, 200–400 mesh). The sample matrix was rinsed off the column in 10 ml 0.5 M HCl–0.5 M HF, followed by another rinse with 10 ml 8 M HCl–0.01 M HF in which significant amounts of Ti, Zr and Hf were eluted. Finally, W was eluted in 15 ml 6 M HCl–1 M HF. The second anion exchange chromatography step[30,33] quantitatively removes high field strength elements (HFSE; Ti, Zr, Hf, Nb) from the W cuts. The samples were evaporated at 200 °C with added $HClO_4$ to destroy organic compounds, re-dissolved in 0.6 M HF–0.2% H_2O_2 and loaded onto pre-cleaned BioRad Polyprep columns filled with 1 ml anion exchange resin (BioRad AG1 × 8, 200–400 mesh). Titanium, Zr and Hf were rinsed off the column with 10 ml 1 M HCl–2% H_2O_2, followed by 10 ml 8 M HCl–0.01 M HF. Finally, W was eluted in 8.5 ml 6 M HCl–1 M HF. The W cuts were evaporated to dryness with added $HClO_4$ (200 °C), converted, and re-dissolved in 0.56 M HNO_3–0.24 M HF measurement solutions. The chemical separation of Hf and W for the spiked aliquots was accomplished using ion exchange chromatography techniques described previously[31]. Total procedural blanks were ~50–300 pg for the W isotope composition analyses, and insignificant given the amounts of W in our samples ($W_{sample}/W_{blank} \approx$ 250–2,000).

Procedures for W isotope measurements by MC-ICPMS. The W isotope measurements were performed using a ThermoScientific Neptune Plus MC-ICPMS in the Institut für Planetologie at the University of Münster. The analytical protocol for high-precision W isotope analyses is based on previously reported procedures[12,33,34]. Samples and standards for W isotope analyses were introduced using an ESI self-aspirating PFA nebulizer (50–60 µl min^{-1}) connected to a Cetac Aridus II desolvator system. Measurements were performed in low-resolution mode using Jet sampler and X-skimmer cones. All four major W isotopes (^{182}W, ^{183}W, ^{184}W, ^{186}W) were measured simultaneously. Total ion beams of ~$(2.0–3.2) \times 10^{-10}$ were obtained for a ~30 p.p.b. W standard solution at an uptake rate of ~60 µl min^{-1}. Electronic baselines were obtained before each sample measurement by deflecting the beam using the electrostatic analyser for 60 s and then subtracted from sample signal intensities. A single W isotope measurement comprised 200 cycles of 4.2 s integration time each. Most samples were measured at least twice, or more often depending on the amount of W that was available for analysis (Extended Data Table 2). Small isobaric interferences from ^{184}Os and ^{186}Os on W isotope ratios were corrected by monitoring interference-free ^{188}Os, and were generally much smaller than 5 p.p.m. Only one sample (68115, BG04) required a slightly larger interference correction of ~15 p.p.m. on ε^{182}W (6/4). Instrumental mass bias was corrected by normalization to either $^{186}W/^{183}W = 1.9859$ (denoted '6/3') or $^{186}W/^{184}W = 0.92767$ (denoted '6/4') using the exponential law. The W isotope analyses of samples were bracketed by measurements of terrestrial solution standards (Alfa Aesar) and results are reported as ε-unit (that is, 0.01%) deviations from the mean values of the bracketing standards, whose concentrations match those of the sample solutions to within less than ~20%. The reported ε^{i}W in Extended Data Table 2 represent the mean of pooled solution replicates ($N = 1–5$) together with their associated external uncertainties (see below).

Accuracy and precision of W isotope measurements. The accuracy and reproducibility of our analytical routine were assessed by repeated analyses of terrestrial rock standards (BHVO-2, BCR-2, AGV-2) whose W concentrations were similar to, or slightly lower than, those of the investigated lunar samples. In each analytical session, separate digestions of these standards were processed through the full chemical separation procedure and analysed alongside the lunar samples. The measurements of the terrestrial standards yield precise ε^{182}W values that are indistinguishable from the value of the terrestrial solution standard (Extended Data Fig. 1, Extended Data Table 1). Reported uncertainties on ε^{182}W of lunar samples are based either on the 2 s.d. obtained for terrestrial standards (in the case $N < 4$), or on the 95% confidence interval of the mean obtained for pooled solution replicates of sample analyses (that is, according to (s.d. × $t_{95\%\ conf.,\ N\text{-}1}$)/$\sqrt{N}$). The latter is justified given that the mean ε^{182}W (6/4) obtained for the terrestrial rock standards yields ε^{182}W (6/4) = 0.00 ± 0.02 (95% conf., $N = 37$), demonstrating the high level of accuracy of the W isotope measurements. Some standard (and sample) analyses showed small anomalies for normalizations involving ^{183}W, including excesses in $\varepsilon^{182/183}$W (6/3) (up to +0.22) and in ε^{184}W (6/3) (up to +0.13), and deficits in ε^{183}W (6/4) (up to −0.19) (Extended Data Tables 1, 2). These coupled ε^{182}W−ε^{183}W systematics have previously been observed in high-precision MC-ICPMS studies for terrestrial standards as well as for silicate rock and iron meteorite samples[5,12,32–34], and are attributed to a mass-independent W isotope fractionation that exclusively affects ^{183}W and that is thought to be induced by W-loss during re-dissolution of the samples in Savillex beakers. The measured $\varepsilon^{182/183}$W (6/3) compositions of terrestrial standards and lunar samples can be corrected for the analytical effect on ^{183}W using different normalization schemes for W isotope measurements and the results obtained for the terrestrial standard[5,12,32–34], according to $\varepsilon^{182/183}W\ (6/3)_{corr.} = \varepsilon^{182/183}W\ (6/3)_{meas.} - 2 \times \varepsilon^{184}W\ (6/3)_{meas.}$. The corrected $\varepsilon^{182/183}$W (6/3) values are indistinguishable from and as precise as the measured $\varepsilon^{182/184}$W (6/4), demonstrating that the corrections are accurate (Extended Data Tables 1-2). Note that ε^{182}W (6/4), that is, the value we use throughout this study, is not affected by the ^{183}W-effect. Thus, the ^{183}W-effect does not compromise any of the conclusions drawn from the W isotope data.

HSE concentrations by isotope dilution. The HSE concentrations of three samples (14321, 68115 and 68815) were determined by isotope dilution. The analytical techniques for HSE analyses are based on procedures described elsewhere[16,35,36], and are briefly summarized below. Samples derive from the same sample powders as used for W isotope composition analyses. Approximately 100 mg powdered sample material was weighed into pre-cleaned Carius tubes. Mixed ^{99}Ru–^{105}Pd–^{191}Ir–^{194}Pt and ^{185}Re–^{190}Os spike solutions were subsequently added followed by 1 ml concentrated HCl and 2 ml concentrated HNO_3. Digestion of the samples in the Carius tubes was performed in an oven at 230 °C for 48 h. Osmium was subsequently separated from the sample solutions by solvent extraction into CCl_4 and then back-extracted into HBr[37]. Rhenium, Ru, Pt, Ir and Pd were separated from the sample matrix by cation exchange chromatography (10 ml BioRad 50W-X8, 100–200 mesh). Samples were loaded onto the column in 2.5 ml 0.2 M HCl. The HSE were then eluted immediately in a subsequent rinse with 14 ml 0.2 M HCl. The sample solutions were evaporated to dryness and re-dissolved in 2.5 ml 0.28 M HNO_3 running solutions. All HSE ratios were measured using a ThermoScientific X-series II quadrupole ICPMS at the Institut für Planetologie. Total procedural blanks were ~0.2 pg for Re, <0.1 pg for Os, ~2 pg for Ir, ~4 pg for Ru, ~35 pg for Pt, and ~15 pg for Pd. The corresponding blank corrections were <0.2% for Re, <0.1% for Os, <0.2% for Ir, <0.2% for Ru, <1.5% for Pt and <0.8% for Pd. As the uncertainties of HSE abundances mainly derive from the blank corrections, the external reproducibility was estimated from the difference of maximum and minimum blank corrections, and assuming an uncertainty on the blank of 50%. This yields uncertainties that are better than 1.5% (2σ) for lunar sample analyses.

Pre-exposure ε^{182}W of the bulk silicate Moon. The crystallization of a lunar magma ocean (LMO)[38–40] produced reservoirs having distinct Hf/W ratios[10,11,41,42], but lunar differentiation at ~4.4 Ga (refs 17, 18) occurred too late (that is, after ^{182}Hf extinction) to generate radiogenic ε^{182}W variations within the Moon. This is consistent with the ε^{182}W values of metals from low- and high-Ti mare basalts[10] having no ε^{180}Hf anomalies[13] and, hence, no neutron capture effects (12004: $\varepsilon^{182}W = 0.05 \pm 0.50$ (2 s.d.); 74255: $\varepsilon^{182}W = 0.11 \pm 0.40$ (2 s.d.); see ref. 10), which are indistinguishable from the KREEP value determined here. Mare basalts have very low HSE contents[3,14], indicating minor meteorite contamination with no significant effect on ε^{182}W. Thus, there is no evidence that the pre-exposure ε^{182}W of the mare basalts would be different from that of KREEP. We, therefore, interpret

the more precise pre-exposure $\varepsilon^{182}W = 0.27 \pm 0.04$ of KREEP to represent that of the bulk silicate Moon.

Effect of meteorite contamination on $\varepsilon^{182}W$. The primordial lunar crust typically is largely devoid of HSE and elevated HSE abundances in some lunar samples are interpreted to reflect contamination with meteoritic impact components at the lunar surface[43–47]. As most meteorites have $\varepsilon^{182}W$ values markedly below those of lunar rocks, any meteoritic component can potentially shift the $\varepsilon^{182}W$ of a lunar sample to lower values. Here we quantify the magnitude of such meteoritic contamination on $\varepsilon^{182}W$ for three key samples that have no resolvable Hf isotope anomaly (14321, 68115, 68815). The HSE concentrations of these three samples were determined by isotope dilution (see Methods) and are given in Extended Data Table 3. The CI-chondrite- and Ir-normalized HSE concentrations of the three samples are shown in Extended Data Fig. 2. The three samples show elevated HSE contents and fractionated HSE patterns with suprachondritic ratios of Ru/Ir, Pt/Ir, Pd/Ir and Re/Os and slightly subchondritic Os/Ir. Such HSE patterns have previously been documented for Apollo 16 impact-melt rocks and probably reflect a mixture of IVA iron-meteorite-like (30%) and carbonaceous chondrite-like (70%) impactor components[47]. Here we assume that this mixture of impactor components had the following composition: [Ir] = 751 p.p.b., [W] = 234 p.p.b., and a $\varepsilon^{182}W$ value of −2.38 (ref. 12, 47, 48). Corrections of measured $\varepsilon^{182}W$ for meteoritic contamination were made using this composition and the measured W and Ir concentrations of the samples. The corrections on $\varepsilon^{182}W$ are ~0.04 and ~0.03 for samples 68115 and 68815 (Table 1). Because of its high W concentration (1,902 p.p.b.; Extended Data Table 3), no correction was needed for sample 14321. Its measured $\varepsilon^{182}W$ of $+0.27 \pm 0.04$ (95% confidence interval) thus defines the pre-exposure $\varepsilon^{182}W$ of KREEP directly. For all other samples, the HSE abundances could not be measured directly and previously reported HSE concentration data (if available) were used instead. For these samples the corrections were less than ~0.02 and, hence, insignificant.

Composition of the late veneer. Information about the mass and composition of the late veneer is provided by the relative and absolute HSE abundances and ratios of Se, Te, and S in Earth's primitive upper mantle[2,8]. Although HSE abundances in Earth's mantle are roughly chondritic, some HSE ratios appear to be slightly fractionated. In particular, compared to chondrites the Earth's mantle is characterized by marked excesses in Pd and Ru relative to Pt, Ir and Os (refs 20, 35, 49, 50). Moreover, the $^{187}Os/^{188}Os$ composition of the primitive upper mantle differs from that of carbonaceous chondrites, but is similar to ordinary and enstatite chondrites[2,35,36,51]. In contrast, the Se/Te ratio of the Earth's mantle is similar to that of carbonaceous chondrites, but different from any other group of chondrites[19]. These contrasting observations as well as the fractionated HSE pattern of the Earth's mantle can be reconciled if the late veneer consisted of carbonaceous chondrites with a minor fraction of differentiated, iron-meteorite-like material[35,36,47]. Here we adopt a mixture of carbonaceous (CI+CM+CV) chondrite material (80%) with an added differentiated IVA-like iron-meteorite component (20%) to represent the composition of the late veneer as previously suggested for late-accreted material on the Moon[47]. This late veneer composition corresponds to a late veneer mass of ~0.35% Earth masses. Alternative late veneer compositions may explain some but not all of the aforementioned HSE and chalcogen signatures. For example, an ordinary-chondrite-like late veneer would explain the $^{187}Os/^{188}Os$ of the BSE, but not its suprachondritic Ru/Ir and Pd/Ir and its Se–Te systematics. Similarly, although a purely carbonaceous-chondrite-like late veneer can explain the Se–Te systematics, it cannot account for the elevated Ru/Ir, Pd/Ir, and the $^{187}Os/^{188}Os$ ratio of the BSE. We, therefore, consider a mixture of carbonaceous-chondrite-like (80%) and iron-meteorite-like (20%) material to be the current best estimate for the composition of the late veneer.

Effect of the late veneer on $\varepsilon^{182}W$ of the BSE. As chondrites and iron meteorites show deficits in $\varepsilon^{182}W$ relative to the BSE, a late veneer with the composition inferred above would have added ^{182}W-depleted material to the BSE. Mass balance calculations indicate that the late veneer lowered the $\varepsilon^{182}W$ of the pre-late-veneer BSE by 0.16–0.38 (Extended Data Table 4, Fig. 1). The effect of the late veneer on $\varepsilon^{182}W$ of the BSE does not change significantly for alternative assumed late veneer compositions and proportions (Extended Data Table 4). Note that the effect is slightly larger for our preferred composition of a mixture of carbonaceous chondrite and iron meteorite than for a late veneer composed entirely of known groups of chondrites, because the presence of W-rich and ^{182}W-depleted iron meteorite material results in a higher W concentration of ~200 p.p.b. and a more negative $\varepsilon^{182}W$ of about −2.6 for the late veneer (using W concentrations of ~113 p.p.b. for CI chondrites[31], ~130 p.p.b. for CM chondrites[31], ~170 p.p.b. for CV chondrites[31], and 480 p.p.b. for the IVA iron meteorites[48], and $\varepsilon^{182}W$ values of −2.2 for CI chondrites, −1.75 for CM chondrites, −2.0 for CV chondrites and −3.3 for IVA iron meteorites[12,31]). For the present-day BSE we used a W concentration of 13 ± 5 p.p.b. (2σ), which is based on the W/U ratio of the BSE of 0.64 ± 0.05 (2 s.e., $N = 86$)[52] and assuming a U concentration for the BSE of 20 ± 8 p.p.b. (2σ)[53–55]. The W concentration of the BSE of 13 ± 5 p.p.b. (2σ) used here is in good agreement with an independent recent estimate of ~12 p.p.b. (ref. 56). The $\varepsilon^{182}W$ of the present-day BSE is 0 by definition.

Effect of giant impact on $\varepsilon^{182}W$ of BSE and Moon. The W isotope compositions of both the pre-late-veneer BSE and the Moon reflect specific mixtures of the same three components: (1) proto-Earth mantle, (2) impactor mantle, and (3) impactor core. Using simple mass balance calculations we demonstrate that the giant impact most probably should have produced distinct $\varepsilon^{182}W$ of the pre-late-veneer BSE and the Moon, for two main reasons. First, the giant impact would have modified the $\varepsilon^{182}W$ of the proto-Earth's mantle, but the material forming the Moon would most probably have been ejected earlier, that is, before the impactor material could have equilibrated fully with the Earth's mantle[1,26,28]. Second, some impactor core material should be present in the lunar accretion disk, and this core material would have had a strong effect on the $\varepsilon^{182}W$ of the bulk Moon. Extended Data Fig. 3 shows the effects of the giant impact on $\varepsilon^{182}W$ of the BSE, plotted as a function of the mass fraction of the impactor relative to Earth's mass ($M_{Imp}/M_{\oplus}$). Shown are the effects for two different impactor compositions, Mars-like or Vesta-like. In terms of their Hf–W systematics, Mars (low mantle Hf/W and $\varepsilon^{182}W$) and Vesta (high mantle Hf/W and radiogenic $\varepsilon^{182}W$) may be considered end members among (known) differentiated planetary bodies in the inner Solar System. The $\varepsilon^{182}W$ of the proto-Earth's mantle is set to zero in the calculations, so that the calculated effects show the difference in $\varepsilon^{182}W$ between the pre- and post-giant impact BSE. Note that assuming a Mars-like impactor represents the end member case of very similar $\varepsilon^{182}W$ in impactor and proto-Earth's mantle, whereas assuming a Vesta-like impactor is the end member case of very different $\varepsilon^{182}W$ in impactor and proto-Earth's mantle. While material from the impactor mantle is directly added to the proto-Earth's mantle, impactor core material is divided between a fraction k that chemically equilibrates with the proto-Earth's mantle and a fraction $(1 - k)$ that directly joins Earth's core without any prior equilibration. Our calculations show that in most cases the giant impact induces a significant shift in the $\varepsilon^{182}W$ value of the BSE, that is, the pre- and post-giant impact $\varepsilon^{182}W$ values of the BSE are probably different (Extended Data Fig. 3). Consequently, even if the Moon predominantly consists of proto-Earth mantle material—as in some recent models of the giant impact[26,27,28]—an $\varepsilon^{182}W$ difference between the BSE and the Moon would be expected. The smallest giant-impact-induced $\varepsilon^{182}W$ shifts are observed for a Mars-like impactor and small impactor-to-Earth ratios. However, even in this case the shift of the BSE $\varepsilon^{182}W$ value would only be small for very low values of k, that is, for low degrees of equilibration of the impactor core with proto-Earth's mantle. For small impactors the degree of equilibration is expected to be high, however[57]. Thus, even the addition of a small impactor having an $\varepsilon^{182}W$ value similar to that of the proto-Earth's mantle would probably induce a significant shift in the $\varepsilon^{182}W$ value of the BSE. Nevertheless, our calculations show that regardless of the $\varepsilon^{182}W$ of the impactor mantle, a specific combination of impactor composition and degree of equilibration of impactor with proto-Earth's mantle can result in no measurable change of $\varepsilon^{182}W$ in the BSE (Extended Data Fig. 3). However, such specific combinations are low-probability cases and it seems far more likely that the giant impact significantly modified the $\varepsilon^{182}W$ of the proto-Earth's mantle.

Another reason why the ^{182}W similarity between the Moon and the pre-late-veneer BSE is remarkable relates to the prediction of most giant-impact simulations that a small fraction of impactor core material is present in the lunar accretion disk[1,26,28]. This material can also account for the presence of a small lunar core[58,59], which otherwise might be difficult to explain. Owing to its high W content and presumably unradiogenic $\varepsilon^{182}W$, the addition of even minute amounts of impactor core material will significantly lower the $\varepsilon^{182}W$ of the proto-lunar material (Extended Data Fig. 4). For a possible range of impactor core compositions and assuming 2.5% impactor core material in the lunar disk (that is, equivalent to the estimated size of the lunar core), the $\varepsilon^{182}W$ of the proto-lunar material would have changed by at least 0.7 but more probably by several ε-units (Extended Data Fig. 4). This effect is large compared to the very close agreement of the pre-late-veneer $\varepsilon^{182}W$ of the BSE and the $\varepsilon^{182}W$ of the Moon.

In summary, both the presence of impactor core material within the lunar accretion disk as well as the effects of the giant impact on the $\varepsilon^{182}W$ of the proto-Earth's mantle are likely to have produced ^{182}W variations in the ε-unit range, yet the $\varepsilon^{182}W$ value of the pre-late-veneer BSE and our newly defined $\varepsilon^{182}W$ value for the Moon are similar to within ~10 p.p.m. It remains possible to explain this similarity by a very specific combination of several parameters[25], including (1) specific compositions of impactor mantle, impactor core and proto-Earth's mantle, (2) degree of re-equilibration of impactor core material within the proto-Earth's mantle, and (3) a particular fraction of impactor core material in the lunar accretion disk. Yet, this would imply that the high degree of similarity in $\varepsilon^{182}W$ of the pre-late-veneer BSE and the Moon is purely coincidental, which seems highly unlikely.

Sample size. No statistical methods were used to predetermine sample size.

30. Kleine, T., Hans, U., Irving, A. J. & Bourdon, B. Chronology of the angrite parent body and implications for core formation in protoplanets. *Geochim. Cosmochim. Acta* **84,** 186–203 (2012).
31. Kleine, T., Mezger, K., Münker, C., Palme, H. & Bischoff, A. ^{182}Hf-^{182}W isotope systematics of chondrites, eucrites, and martian meteorites: chronology of core formation and early mantle differentiation in Vesta and Mars. *Geochim. Cosmochim. Acta* **68,** 2935–2946 (2004).
32. Kruijer, T. S. *et al.* Hf–W chronometry of core formation in planetesimals inferred from weakly irradiated iron meteorites. *Geochim. Cosmochim. Acta* **99,** 287–304 (2012).
33. Kruijer, T. S., Kleine, T., Fischer-Gödde, M., Burkhardt, C. & Wieler, R. Nucleosynthetic W isotope anomalies and the Hf-W chronometry of Ca-Al-rich inclusions. *Earth Planet. Sci. Lett.* **403,** 317–327 (2014).
34. Kruijer, T. S. *et al.* Neutron capture on Pt isotopes in iron meteorites and the Hf–W chronology of core formation in planetesimals. *Earth Planet. Sci. Lett.* **361,** 162–172 (2013).
35. Fischer-Gödde, M., Becker, H. & Wombacher, F. Rhodium, gold and other highly siderophile elements in orogenic peridotites and peridotite xenoliths. *Chem. Geol.* **280,** 365–383 (2011).
36. Fischer-Gödde, M., Becker, H. & Wombacher, F. Rhodium, gold and other highly siderophile element abundances in chondritic meteorites. *Geochim. Cosmochim. Acta* **74,** 356–379 (2010).
37. Cohen, A. S. & Waters, F. G. Separation of osmium from geological materials by solvent extraction for analysis by thermal ionisation mass spectrometry. *Anal. Chim. Acta* **332,** 269–275 (1996).
38. Wood, J. A., Dickey, J. S., Marvin, U. B. & Powell, B. N. Lunar anorthosites and a geophysical model of the Moon. *Proc. Apollo 11 Lunar Sci. Conf.* **1,** 965–988 (1970).
39. Taylor, S. R. & Jakeš, P. The geochemical evolution of the Moon. *Proc. Fifth Lunar Conf.* **2,** 1287–1305 (1974).
40. Warren, P. H. & Wasson, J. T. The origin of KREEP. *Rev. Geophys.* **17,** 73–88 (1979).
41. Righter, K. & Shearer, C. K. Magmatic fractionation of Hf and W: constraints on the timing of core formation and differentiation in the Moon and Mars. *Geochim. Cosmochim. Acta* **67,** 2497–2507 (2003).
42. Münker, C. A high field strength element perspective on early lunar differentiation. *Geochim. Cosmochim. Acta* **74,** 7340–7361 (2010).
43. Morgan, J. W., Walker, R. J., Brandon, A. D. & Horan, M. F. Siderophile elements in Earth's upper mantle and lunar breccias: data synthesis suggests manifestations of the same late influx. *Meteorit. Planet. Sci.* **36,** 1257–1275 (2001).
44. Korotev, R. L. The meteorite component of Apollo 16 noritic impact melt breccias. *J. Geophys. Res.* **92,** E491 (1987).
45. Puchtel, I. S., Walker, R. J., James, O. B. & Kring, D. A. Osmium isotope and highly siderophile element systematics of lunar impact melt breccias: implications for the late accretion history of the Moon and Earth. *Geochim. Cosmochim. Acta* **72,** 3022–3042 (2008).
46. Norman, M. D., Bennett, V. C. & Ryder, G. Targeting the impactors?: siderophile element signatures of lunar impact melts from Serenitatis. *Geochim. Cosmochim. Acta* **202,** 217–228 (2002).
47. Fischer-Gödde, M. & Becker, H. Osmium isotope and highly siderophile element constraints on ages and nature of meteoritic components in ancient lunar impact rocks. *Geochim. Cosmochim. Acta* **77,** 135–156 (2012).
48. McCoy, T. J. *et al.* Group IVA irons: new constraints on the crystallization and cooling history of an asteroidal core with a complex history. *Geochim. Cosmochim. Acta* **75,** 6821–6843 (2011).
49. Pattou, L., Lorand, J. P. & Gros, M. Non-chondritic platinum-group element ratios in the Earth's mantle. *Nature* **379,** 712–715 (1996).
50. Horan, M. Highly siderophile elements in chondrites. *Chem. Geol.* **196,** 27–42 (2003).
51. Meisel, T., Walker, R. J., Irving, A. J. & Lorand, J.-P. Osmium isotopic compositions of mantle xenoliths: a global perspective. *Geochim. Cosmochim. Acta* **65,** 1311–1323 (2001).
52. Arevalo, R. & McDonough, W. F. Tungsten geochemistry and implications for understanding the Earth's interior. *Earth Planet. Sci. Lett.* **272,** 656–665 (2008).
53. McDonough, W. F. & Sun, S.-s. The composition of the Earth. *Chem. Geol.* **120,** 223–253 (1995).
54. Lyubetskaya, T. & Korenaga, J. Chemical composition of Earth's primitive mantle and its variance: 1. Method and results. *J. Geophys. Res.* **112,** B03211 (2007).
55. Palme, H. & O'Neill, H. S. C. *Cosmochemical Estimates of Mantle Composition. Treatise on Geochemistry* (2nd edn), **3,** 1–39 (Elsevier, 2014).
56. König, S. *et al.* The Earth's tungsten budget during mantle melting and crust formation. *Geochim. Cosmochim. Acta* **75,** 2119–2136 (2011).
57. Dahl, T. W. & Stevenson, D. J. Turbulent mixing of metal and silicate during planet accretion — And interpretation of the Hf–W chronometer. *Earth Planet. Sci. Lett.* **295,** 177–186 (2010).
58. Khan, A., Maclennan, J., Taylor, S. R. & Connolly, J. A. D. Are the Earth and the Moon compositionally alike? Inferences on lunar composition and implications for lunar origin and evolution from geophysical modeling. *J. Geophys. Res.* **111,** E05005 (2006).
59. Weber, R. C., Lin, P.-Y., Garnero, E. J., Williams, Q. & Lognonné, P. Seismic detection of the lunar core. *Science* **331,** 309–312 (2011).
60. Palme, H. Lodders, K. & Jones, A. *Solar System Abundances of the Elements. Treatise on Geochemistry* (2nd edn), **2,** 15–36 (Elsevier, 2014).
61. Cottrell, E., Walter, M. J. & Walker, D. Metal–silicate partitioning of tungsten at high pressure and temperature: Implications for equilibrium core formation in Earth. *Earth Planet. Sci. Lett.* **281,** 275–287 (2009).

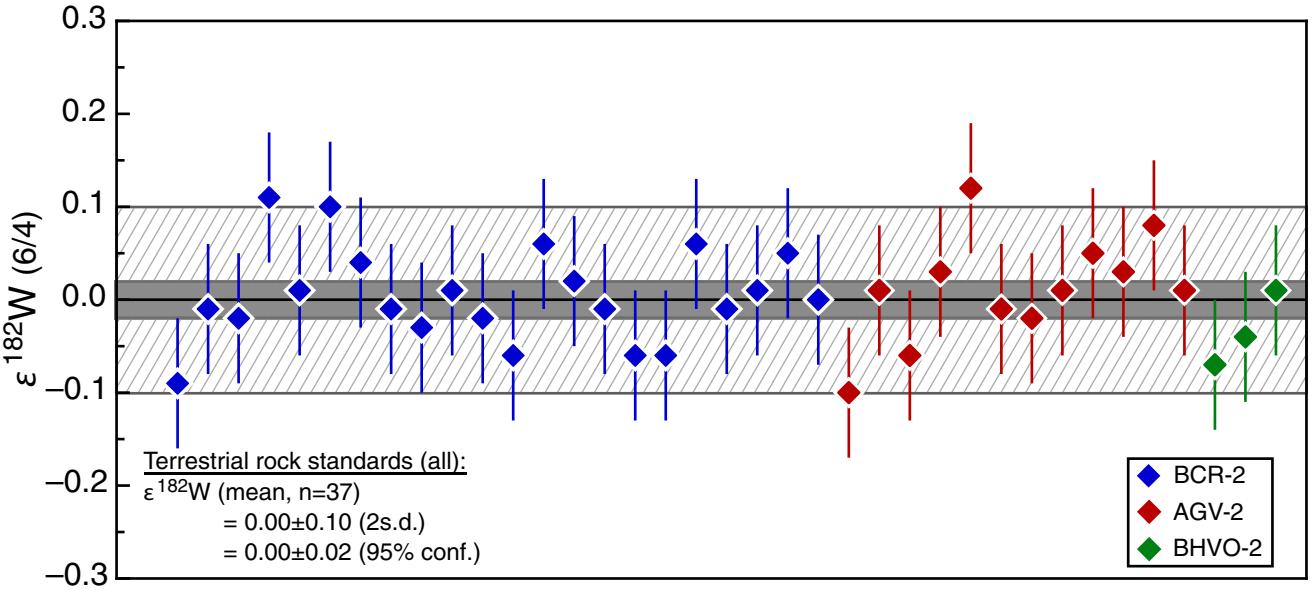

Extended Data Figure 1 | Compilation of $\varepsilon^{182}W$ results obtained for three terrestrial rock standards, BCR-2, AGV-2 and BHVO-2. Each of these standards was analysed together with the lunar samples. $\varepsilon^{182}W$ (6/4) indicates that the data have been normalized to $^{186}W/^{184}W = 0.92767$ (denoted '6/4'); see Methods for details. Error bars indicate internal uncertainties (2 s.e.) for a single measurement of 200 cycles. The external uncertainty (2 s.d.), as inferred from replicate standard analyses, is shown as a grey-hatched area, and the corresponding 95% confidence interval of 2 p.p.m. as a solid grey area.

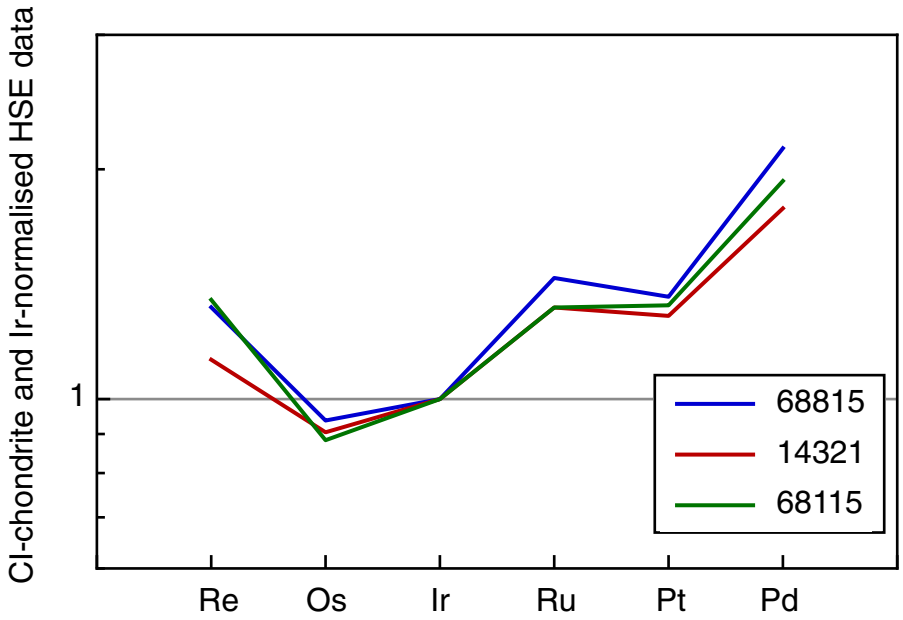

Extended Data Figure 2 | CI-chondrite-normalized and Ir-normalized HSE concentrations of lunar samples 14321, 68115, and 68815. HSE concentrations are first normalized to chondritic abundances, then to the chondrite normalized Ir concentration. Corresponding HSE concentrations are given in Extended Data Table 3.

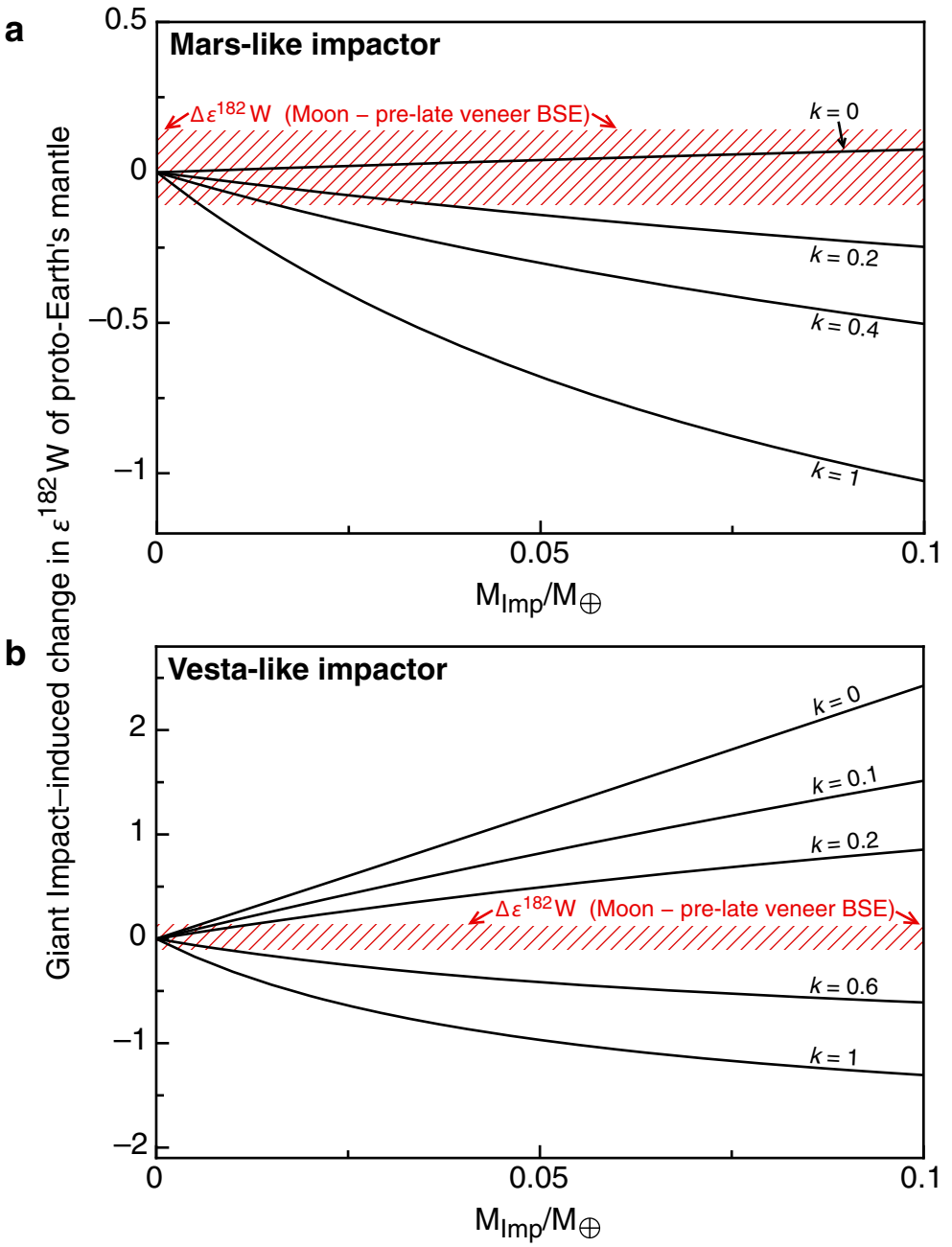

Extended Data Figure 3 | Change of ε^{182}W of the proto-Earth's mantle through addition of impactor material. The varying amounts of impactor material are given as $M_{imp}/M_{\oplus}$ where M_{imp} and $M_{\oplus}$ are respectively the mass of impactor material and the Earth's mass. Hatched area (red) shows the maximum possible difference between the (eventual) ε^{182}W of the pre-late-veneer BSE and the Moon, as inferred from the difference between the lunar pre-exposure ε^{182}W value ($+0.27 \pm 0.04$) and that calculated for the BSE before addition of the late veneer ($+0.22^{+0.16}_{-0.06}$). Shown are the effects of different degrees of equilibration of the impactor core with the proto-Earth's mantle, from full ($k = 1$) to no equilibration ($k = 0$) and for two different impactor compositions: **a**, volatile-element-enriched 'Mars-like' and **b**, volatile-element-depleted 'Vesta-like'. In both cases the impactor was assumed to have core and mantle fractions of 32% and 68%, identical to the Earth. For the (proto-)Earth's mantle we used a W concentration of 13 ± 5 p.p.b. (2σ) (see Methods); its ε^{182}W is set to zero. For the Mars-like impactor, CI-chondritic Hf (107 p.p.b.) and W (93 p.p.b.) concentrations[60] were assumed. As core formation in this impactor would have occurred under more oxidizing conditions, we chose a relatively low metal–silicate partition coefficient[61] for W of $D_W = 6$, which yields a relatively high W concentration of $[W]_{IM} = 41$ p.p.b. in the impactor mantle (and a low Hf/W of 4.4), and a correspondingly low W concentration of $[W]_{IC} = 205$ p.p.b. in the core. The metal–silicate differentiation age was set to 9 Myr after CAI formation, resulting in a ε^{182}W of −2.7 in the metal core, and a ε^{182}W of +0.32 in the silicate mantle (calculated using a Solar System initial $^{182}Hf/^{180}Hf_i$ of $(1.018 \pm 0.043) \times 10^{-4}$; ref. 33). For the Vesta-like impactor we assumed CV-chondritic Hf (200 p.p.b.) and W (175 p.p.b.) concentrations[31]. Core formation in this impactor would have occurred under more reduced conditions, so the metal–silicate partition coefficient for W was set to a relatively high value ($D_W = 42$)[61]. This yields a low W concentration in the silicate mantle ($[W]_{IM} = 12$ p.p.b.), a high Hf/W of 25 in the silicate mantle, and a relatively high W concentration in the metal core ($[W]_{IC} = 522$ p.p.b.) The metal–silicate differentiation age was set to 2 Myr after CAI formation, resulting in a $\varepsilon^{182}W_{IC}$ of −3.3 in the metal core, and a $\varepsilon^{182}W_{IM}$ of +27 in the silicate mantle.

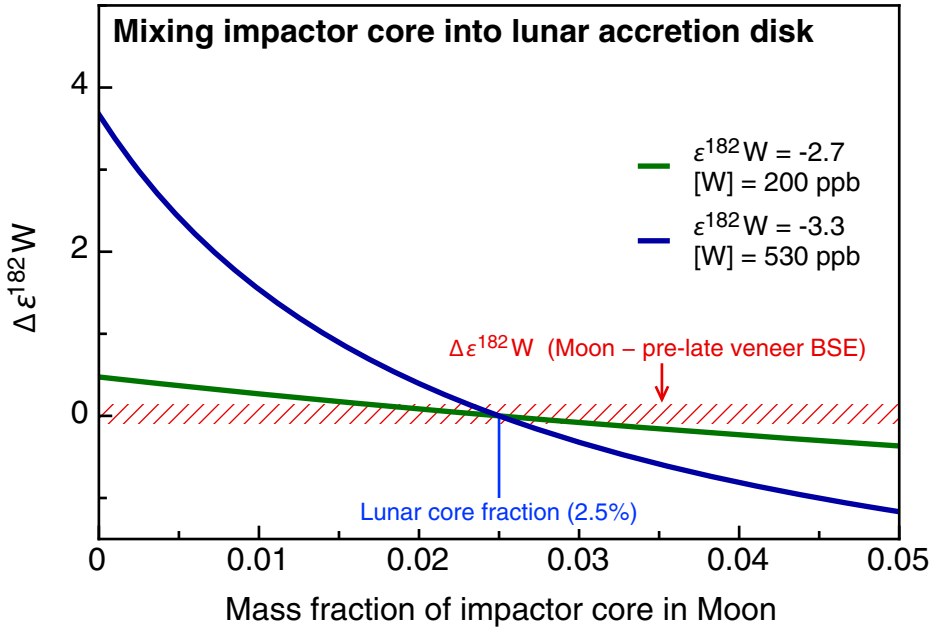

Extended Data Figure 4 | Effect of mixing impactor core into the lunar accretion disk on the ε^{182}W of the Moon. Shown are the effects on ε^{182}W for two different impactor compositions (green and blue lines). Hatched area (red) shows the maximum possible difference between the (eventual) ε^{182}W of Earth and Moon as inferred from the difference between the lunar pre-exposure ε^{182}W value ($+0.27 \pm 0.04$) and that calculated for the BSE before addition of late veneer ($+0.22^{+0.16}_{-0.06}$). In the mass balance we considered the same two impactor compositions as used in the mass balance shown in Extended Data Fig. 3, including (1) an (oxidized) volatile-element-rich impactor (green line), and (2) a (reduced) volatile-element-poor impactor (blue line). We used the same Hf and W concentrations, partition coefficients, core and mantle fractions, and differentiation ages, so the resulting Hf/W and ε^{182}W values of impactor mantle and core are identical to those above. The amount of impactor core material currently present in the Moon is assumed to be equivalent to the lunar core fraction, that is, 2.5% of its mass. For this reason the mixing lines intersect the ordinate ($\Delta\varepsilon^{182}W = 0$) at 2.5%. For simplicity we assume the proportion of impactor material present in the Moon to be 80%, that is, consistent with most 'canonical' giant-impact models[1].

Extended Data Table 1 | Tungsten isotope data for terrestrial rock standards

Sample	ID	$\varepsilon^{182/183}$W (6/3) (±2σ)	$\varepsilon^{182/184}$W (6/4) (±2σ)	$\varepsilon^{183/184}$W (6/4) (±2σ)	$\varepsilon^{184/183}$W (6/3) (±2σ)	$\varepsilon^{182/183}W_{corr.}$ (6/3) (±2σ)[a]
BCR-2	BB03	-0.04 ± 0.06	-0.05 ± 0.08	0.00 ± 0.06	0.00 ± 0.04	-0.05 ± 0.10
	BB03	0.18 ± 0.06	-0.01 ± 0.08	-0.14 ± 0.06	0.09 ± 0.04	-0.01 ± 0.10
	BB04	0.02 ± 0.06	-0.02 ± 0.08	-0.03 ± 0.06	0.02 ± 0.04	-0.02 ± 0.10
	BB04	0.03 ± 0.06	0.11 ± 0.08	0.06 ± 0.06	-0.04 ± 0.04	0.11 ± 0.10
	BF07	-0.03 ± 0.06	0.04 ± 0.08	-0.03 ± 0.06	-0.06 ± 0.04	0.09 ± 0.10
	BF07	0.20 ± 0.06	-0.06 ± 0.08	-0.19 ± 0.06	0.13 ± 0.04	-0.06 ± 0.10
	BF07	0.22 ± 0.06	0.10 ± 0.08	-0.09 ± 0.06	0.06 ± 0.04	0.10 ± 0.10
	BG05	0.17 ± 0.06	0.01 ± 0.08	-0.12 ± 0.06	0.08 ± 0.04	0.02 ± 0.10
	BG05	0.10 ± 0.06	-0.04 ± 0.08	-0.11 ± 0.06	0.07 ± 0.04	-0.04 ± 0.10
	BG05	0.05 ± 0.06	0.02 ± 0.08	-0.03 ± 0.06	0.02 ± 0.04	0.01 ± 0.10
	BD03	0.15 ± 0.06	-0.06 ± 0.08	-0.16 ± 0.06	0.10 ± 0.04	-0.06 ± 0.10
	BD03	0.17 ± 0.06	0.01 ± 0.08	-0.12 ± 0.06	0.08 ± 0.04	0.01 ± 0.10
	BD07	-0.01 ± 0.06	0.04 ± 0.08	0.04 ± 0.06	-0.03 ± 0.04	0.04 ± 0.10
	BD07	0.14 ± 0.06	0.02 ± 0.08	-0.09 ± 0.06	0.06 ± 0.04	0.02 ± 0.10
	BD02	-0.04 ± 0.06	-0.05 ± 0.08	-0.01 ± 0.06	0.01 ± 0.04	-0.05 ± 0.10
	BA05	0.01 ± 0.06	-0.04 ± 0.08	-0.04 ± 0.06	0.03 ± 0.04	-0.04 ± 0.10
	BA05	0.04 ± 0.06	-0.06 ± 0.08	-0.02 ± 0.06	0.01 ± 0.04	0.02 ± 0.10
	BI05	0.11 ± 0.06	0.05 ± 0.08	-0.05 ± 0.06	0.03 ± 0.04	0.05 ± 0.10
	BI05	0.15 ± 0.06	0.01 ± 0.08	-0.11 ± 0.06	0.07 ± 0.04	0.01 ± 0.10
	BI05	0.16 ± 0.06	-0.04 ± 0.08	-0.15 ± 0.06	0.10 ± 0.04	-0.04 ± 0.10
	BL04	0.11 ± 0.06	0.06 ± 0.08	-0.04 ± 0.06	0.02 ± 0.04	0.06 ± 0.10
	BL04	0.20 ± 0.06	0.01 ± 0.08	-0.14 ± 0.06	0.09 ± 0.04	0.01 ± 0.10
AGV-2	BA06	0.03 ± 0.06	-0.06 ± 0.08	-0.07 ± 0.06	0.05 ± 0.04	-0.06 ± 0.10
	BA06	0.04 ± 0.06	-0.03 ± 0.08	-0.05 ± 0.06	0.04 ± 0.04	-0.03 ± 0.10
	BD04	0.21 ± 0.06	-0.06 ± 0.08	-0.21 ± 0.06	0.14 ± 0.04	-0.06 ± 0.10
	BD04	0.07 ± 0.06	0.01 ± 0.08	-0.05 ± 0.06	0.03 ± 0.04	0.01 ± 0.10
	BD04	0.22 ± 0.06	0.11 ± 0.08	-0.09 ± 0.06	0.06 ± 0.04	0.11 ± 0.10
	BD05	0.07 ± 0.06	-0.04 ± 0.08	-0.08 ± 0.06	0.06 ± 0.04	-0.04 ± 0.10
	BD05	0.12 ± 0.06	-0.03 ± 0.08	-0.11 ± 0.06	0.07 ± 0.04	-0.03 ± 0.10
	BD06	-0.01 ± 0.06	-0.01 ± 0.08	0.00 ± 0.06	0.00 ± 0.04	-0.01 ± 0.10
	BD06	0.13 ± 0.06	0.03 ± 0.08	-0.07 ± 0.06	0.05 ± 0.04	0.03 ± 0.10
	BL05	0.14 ± 0.06	0.05 ± 0.08	-0.06 ± 0.06	0.04 ± 0.04	0.05 ± 0.10
	BL05	0.22 ± 0.06	0.07 ± 0.08	-0.11 ± 0.06	0.08 ± 0.04	0.07 ± 0.10
	BL05	0.11 ± 0.06	-0.02 ± 0.08	-0.10 ± 0.06	0.07 ± 0.04	-0.02 ± 0.10
BHVO-2	BD01	0.10 ± 0.06	-0.06 ± 0.08	-0.12 ± 0.06	0.08 ± 0.04	-0.06 ± 0.10
	BC05	0.07 ± 0.06	-0.08 ± 0.08	-0.12 ± 0.06	0.08 ± 0.04	-0.08 ± 0.10
	BL06	-0.01 ± 0.06	0.04 ± 0.08	0.04 ± 0.06	-0.02 ± 0.04	0.04 ± 0.10
Mean all	(±2s.d., *N*=37)	0.10 ± 0.16	0.00 ± 0.10	-0.07 ± 0.12	0.05 ± 0.09	0.00 ± 0.10
	(±95% conf.)	± 0.03	± 0.02	± 0.01	± 0.02	± 0.02

Instrumental mass fractionation was corrected using the exponential law by internal normalization to $^{186}W/^{184}W = 0.92767$ (6/4) or $^{186}W/^{183}W = 1.98594$ (6/3). Terrestrial rock standards (~0.2 g BCR-2, AGV-2 or BHVO-2) were digested, processed and analysed together with the lunar samples. Each line represents a single measurement of 200 cycles (4.2 s each). Quoted uncertainties of individual runs are based on within-run statistics and represent two standard errors of the mean (2 s.e.). [a]Corrected for an analytical effect on ^{183}W according to $\varepsilon^{182}W\,(6/3)_{corr.} = \varepsilon^{182}W\,(6/3)_{meas.} - 2 \times \varepsilon^{184}W\,(6/3)_{meas.}$. The added uncertainty induced by this correction is included in the reported uncertainties of individual $\varepsilon^{182}W_{corr.}$ (6/3) values.

Extended Data Table 2 | Tungsten isotope data for KREEP-rich samples

Sample	Specific	ID		$\varepsilon^{182/183}$W (6/3) (±2σ)	$\varepsilon^{182/184}$W (6/4) (±2σ)	$\varepsilon^{183/184}$W (6/4) (±2σ)	$\varepsilon^{184/183}$W (6/3) (±2σ)	$\varepsilon^{182/183}W_{corr.}$ (6/3) (±2σ)[a]
14321	1827	BF01		0.70 ± 0.11	0.34 ± 0.13	-0.25 ± 0.11	0.17 ± 0.08	0.37 ± 0.19
14321	1827	BG04		0.25 ± 0.08	0.24 ± 0.11	0.00 ± 0.08	-0.01 ± 0.05	0.27 ± 0.13
14321	1827		Mean (2s.d.; *N*=2)	0.47 ± 0.15	0.29 ± 0.10	-0.12 ± 0.12	0.08 ± 0.08	0.32 ± 0.10
14321	1856	BL02		0.33 ± 0.06	0.30 ± 0.08	-0.02 ± 0.06	0.01 ± 0.04	0.30 ± 0.10
14321	1856	BL02		0.26 ± 0.07	0.30 ± 0.07	0.03 ± 0.06	-0.02 ± 0.04	0.30 ± 0.11
14321	1856	BL02		0.40 ± 0.07	0.20 ± 0.08	-0.15 ± 0.07	0.10 ± 0.04	0.20 ± 0.11
14321	1856	BL02		0.36 ± 0.07	0.32 ± 0.09	-0.03 ± 0.06	0.02 ± 0.04	0.32 ± 0.11
14321	1856	BL02		0.38 ± 0.07	0.27 ± 0.08	-0.09 ± 0.07	0.06 ± 0.04	0.27 ± 0.11
14321	1856	BL02		0.33 ± 0.06	0.23 ± 0.10	-0.08 ± 0.07	0.05 ± 0.04	0.23 ± 0.11
14321	1856		Mean (95% conf.; *N*=6)	0.34 ± 0.05	0.27 ± 0.05	-0.06 ± 0.07	0.04 ± 0.04	0.27 ± 0.05
68115	295	BL01		0.36 ± 0.07	0.26 ± 0.09	-0.07 ± 0.06	0.05 ± 0.04	0.26 ± 0.11
68115	295	BL01		0.36 ± 0.06	0.22 ± 0.08	-0.10 ± 0.06	0.07 ± 0.04	0.22 ± 0.11
68115	295	BL01		0.38 ± 0.07	0.29 ± 0.09	-0.07 ± 0.06	0.05 ± 0.04	0.29 ± 0.11
68115	295	BL01		0.27 ± 0.07	0.20 ± 0.09	-0.05 ± 0.07	0.03 ± 0.05	0.20 ± 0.12
68115	295		Mean (2s.d.; *N*=4)	0.34 ± 0.08	0.24 ± 0.06	-0.07 ± 0.03	0.05 ± 0.02	0.24 ± 0.06
68115	112	BI04		0.34 ± 0.08	0.27 ± 0.12	-0.06 ± 0.09	0.04 ± 0.06	0.27 ± 0.14
68115	112	BD08		0.46 ± 0.17	0.28 ± 0.18	-0.14 ± 0.14	0.09 ± 0.10	0.28 ± 0.26
68115	112	BG03		0.27 ± 0.11	0.28 ± 0.13	-0.01 ± 0.10	0.01 ± 0.07	0.25 ± 0.18
68115	112		Mean (2s.d.; *N*=3)	0.36 ± 0.15	0.27 ± 0.10	-0.07 ± 0.12	0.05 ± 0.08	0.26 ± 0.10
68815	400	BL03		0.38 ± 0.07	0.20 ± 0.09	-0.14 ± 0.07	0.09 ± 0.05	0.20 ± 0.12
68815	400	BL03		0.41 ± 0.07	0.17 ± 0.09	-0.18 ± 0.07	0.12 ± 0.05	0.17 ± 0.12
68815	400		Mean (2s.d.; *N*=2)	0.40 ± 0.15	0.18 ± 0.10	-0.16 ± 0.12	0.11 ± 0.08	0.19 ± 0.13
14163	921	BI03		2.26 ± 0.06	2.30 ± 0.08	0.03 ± 0.06	-0.02 ± 0.04	2.30 ± 0.10
14163	921	BI03		2.32 ± 0.06	2.36 ± 0.08	0.03 ± 0.06	-0.02 ± 0.04	2.36 ± 0.10
14163	921	BI03		2.23 ± 0.06	2.36 ± 0.08	0.10 ± 0.06	-0.07 ± 0.04	2.36 ± 0.10
14163	921	BI03		2.41 ± 0.06	2.36 ± 0.08	-0.04 ± 0.06	0.03 ± 0.04	2.36 ± 0.10
14163	921	BI03		2.43 ± 0.06	2.40 ± 0.08	-0.02 ± 0.06	0.02 ± 0.04	2.40 ± 0.10
14163	921		Mean (*N*=5)	2.33 ± 0.11	2.35 ± 0.04	0.02 ± 0.07	-0.01 ± 0.04	2.35 ± 0.05
12034	120	BF03		1.26 ± 0.07	1.32 ± 0.09	0.05 ± 0.08	-0.03 ± 0.05	1.32 ± 0.12
12034	120	BF03		1.23 ± 0.07	1.25 ± 0.09	0.01 ± 0.08	-0.01 ± 0.05	1.25 ± 0.13
12034	120	BF03		1.18 ± 0.07	1.22 ± 0.10	0.03 ± 0.09	-0.02 ± 0.06	1.22 ± 0.14
12034	120		Mean (*N*=3)	1.22 ± 0.15	1.26 ± 0.10	0.03 ± 0.12	-0.02 ± 0.08	1.26 ± 0.10
14310	676	BF02		1.89 ± 0.08	1.84 ± 0.09	-0.04 ± 0.07	0.03 ± 0.05	1.84 ± 0.12
14310	676	BF02		1.97 ± 0.09	1.90 ± 0.10	-0.05 ± 0.08	0.03 ± 0.06	1.90 ± 0.14
14310	676	BF02		1.93 ± 0.07	1.86 ± 0.10	-0.05 ± 0.09	0.03 ± 0.06	1.86 ± 0.14
14310	676		Mean (*N*=3)	1.93 ± 0.15	1.87 ± 0.10	-0.05 ± 0.12	0.03 ± 0.08	1.87 ± 0.10
62235	122	BG02		1.76 ± 0.07	1.62 ± 0.10	-0.11 ± 0.07	0.07 ± 0.04	1.62 ± 0.11
62235	122	BG02		1.65 ± 0.07	1.64 ± 0.09	0.00 ± 0.07	0.00 ± 0.04	1.64 ± 0.11
62235	122		Mean (*N*=2)	1.70 ± 0.15	1.63 ± 0.10	-0.05 ± 0.12	0.04 ± 0.08	1.63 ± 0.10

Instrumental mass fractionation was corrected using the exponential law by internal normalization to $^{186}W/^{184}W = 0.92767$ (6/4) or $^{186}W/^{183}W = 1.98594$ (6/3). The uncertainties reported for single $\varepsilon^{i}W$ measurements (200 cycles) are derived from internal run statistics and represent the standard error of the mean (2 s.e.). The uncertainties of mean $\varepsilon^{i}W$ values represent the standard deviation (2 s.d.) obtained from replicate analyses of terrestrial rock standards (Extended Data Table 1) in the case $N < 4$, or in the case $N \geq 4$, the 95% confidence intervals of the mean (that is, according to: (s.d. $\times$ $t_{0.95,N-1}$)/$\sqrt{N}$). [a]Corrected for an analytical effect on ^{183}W according to $\varepsilon^{182}W\ (6/3)_{corr.} = \varepsilon^{182}W\ (6/3)_{meas.} - 2 \times \varepsilon^{184}W\ (6/3)_{meas.}$. The added uncertainty induced by this correction is included in the reported uncertainties of individual $\varepsilon^{182}W_{corr.}$ (6/3) values.

Extended Data Table 3 | Hf, W, and HSE concentrations of KREEP-rich samples determined by isotope dilution

Sample	Specific	ID	Hf (ppb)	W (ppb)	$^{180}Hf/^{184}W$ (±2σ)	Re (ppb)	Os (ppb)	Ir (ppb)	Ru (ppb)	Pt (ppb)	Pd (ppb)	Re/Ir	Os/Ir	Ru/Ir	Pt/Ir	Pd/Ir	W/Ir	Impactor[a] (%)
68815	400	BM01	5590	332	19.9 ± 0.2	1.23	10.5	10.6	22.7	29.4	27.4	0.12	1.00	2.15	2.78	2.60	31.4	0.73
14321	1856	BM02	25560	1900	15.9 ± 0.1	0.68	6.61	6.87	13.5	18.0	14.9	0.10	0.96	1.96	2.62	2.17	277	0.47
68115	295	BM03	3824	667	6.76 ± 0.04	3.5	27.3	29.1	57.0	78.7	68.3	0.12	0.94	1.96	2.71	2.35	23.0	2.0

Analytical details of HSE analyses are given in Methods. [a]Percentage of impactor component in lunar rock as inferred from its measured Ir concentration relative to that of the inferred composition of the impactor component.

Extended Data Table 4 | Late veneer (LV) compositions and their effect on the ε^{182}W value of Earth's mantle

	$[W]_{LV}$	$\varepsilon^{182}W_{LV}$	Mass fraction of LV in Earth[a]	pre-LV $\varepsilon^{182}W$[b]	(+)	(-)
CI	113	-2.20	0.0059	0.17	0.29	0.12
CM	127	-1.73	0.0045	0.11	0.19	0.08
CO	169	-1.83	0.0033	0.12	0.20	0.09
CK	199	-2.00	0.0037	0.18	0.30	0.12
CV	171	-1.97	0.0035	0.14	0.23	0.10
CR	165	-1.77	0.0041	0.14	0.24	0.10
Mean carb. chond.	156	-1.89	0.0043	0.15	0.25	0.10
H	178	-2.25	0.0032	0.16	0.28	0.12
L	129	-2.00	0.0044	0.14	0.24	0.10
LL	95	-1.60	0.0074	0.14	0.24	0.10
EH	128	-2.23	0.0045	0.15	0.26	0.11
EL	135	-1.98	0.0041	0.14	0.23	0.10
IVA	482	-3.32	0.0017	0.33	0.56	0.23
80% CC+20% IVA	202	-2.60	0.0034	0.22	0.38	0.16

[a]Fraction of late veneer mass relative to the Earth's mass. [b]Pre-late-veneer $\varepsilon^{182}W$ given relative to the present-day W isotope composition of the modern mantle, and their uncertainties, which are mainly governed by the W concentration of the BSE. Data sources: W concentrations and $\varepsilon^{182}W$ are from refs 12, 31, 48; Ir concentrations are from refs 36, 48, 50). Full details are given in Methods.